Intensive Care Med (2000) 26: 1046–1056

ORIGINAL

J.-J. Rouby
L. Puybasset
P. Cluzel
J. Richecoeur
Q. Lu
P. Grenier
and the CT Scan ARDS Study Group

Regional distribution of gas and tissue in acute respiratory distress syndrome. II. Physiological correlations and definition of an ARDS Severity Score

Received: 12 May 1999
Final revision received: 9 February 2000
Accepted: 10 April 2000

The following members of the CT Scan ARDS Study Group participated in this study: L. Gallart, Servei d'Anestesiologia, Hospital Universitari del Mar, Barcelona, Spain; G.S. Umamaheswara Rao, Department of Anesthesia, National Institute of Mental Health and Neurosciences, Bengalore, India; S. Vieira, Hospital De Clinicas de Porto Allegre, UFRGS, Brasil; L Malbouisson, Department of Anesthesiology, Hospital Das Clinicas, Sao Paulo, Brasil; M.O. Roussat and J.-D. Law-Koune, L. Abdennour, Réanimation Chirurgicale Pierre Viars, Hôpital de La Pitié-Salpêtrière, Paris, France; D. Gava and F. Préteux, Institut National des télécommunications, Evry, France; P. Grenier, Service de Radiologie, Hôpital de la Pitié-Salpétrière.

J.-J. Rouby (✉) · L. Puybasset · P. Cluzel · J. Richecoeur · Q. Lu · P. Grenier
Réanimation Chirurgicale Pierre Viars, Department of Anesthesiology, and the Department of Radiology, Hôpital de la Pitié-Salpetrière, University Pierre et Marie Curie, 47–83 boulevard de l'Hôpital, 75013 Paris, France
e-mail: jjrouby.pitie@invivo.edu
Tel.: + 33-1-42 17 73 00
Fax: + 33-1-42 17 73 26

Present address:
J. Richecoeur
Medical ICU, Pontoise Hospital, Pontoise, France

Abstract *Objectives*: (a) To assess whether differences in lung morphology observed in patients with adult respiratory distress syndrome (ARDS) are associated with differences in cardiorespiratory parameters, lung mechanics, and outcome. (b) To propose a new ARDS Severity Score to identify patients with a high mortality risk.
Design: Prospective study over a 53-month period.
Setting: Fourteen-bed surgical intensive care unit of a university hospital.
Patients and participants: Seventy-one consecutive patients with early ARDS.
Measurements and results: Cardiorespiratory parameters were measured using a Swan-Ganz catheter, the pressure-volume (PV) curve was measured using the gross syringe method, and fast spiral computed tomography (CT) was performed. Patients with diffuse attenuations ($n = 16$) differed from patients with lobar attenuations ($n = 26$) regarding: (a) mortality rate (75 % vs. 42 %, $p = 0.05$), (b) incidence of primary ARDS (82 % vs. 50 %, $p = 0.03$), (c) respiratory compliance (47 ± 12 vs. 64 ± 16 ml per cmH_2O^{-1} $p = 0.04$), and (d) lower inflexion point (8.4 ± 2.0 vs. 4.6 ± 2.0 cmH_2O, $p = 0.001$). A third group of patients with patchy attenuations ($n = 29$) had a mortality rate of 41 %, a respiratory compliance of 56 ± 18 ml per cmH_2O^{-1} and a lower inflexion point of 6.3 ± 2.7 cmH_2O. The bedside chest radiograph accurately assessed lung morphology in only 42 % of the patients. In contrast to the scores based on the bedside chest radiograph, a new ARDS Severity Score based on CT lung morphology and cardiorespiratory parameters identified a subgroup of patients with a high mortality rate (≥ 60 %).
Conclusions: In patients with ARDS, differences in lung morphology are associated with differences in outcome and lung mechanics. A new ARDS Severity Score based on CT lung morphology and cardiorespiratory parameters accurately identified patients with the most severe forms of ARDS and a mortality rate above 60 %.

Key words Adult respiratory distress syndrome · Outcome · Computed tomography · Lung morphology · Lung mechanics · Lung volumes

Introduction

Lungs of patients fulfilling the criteria of the American-European Consensus Conference on ARDS [1] are characterized by an excess of lung tissue and a loss of aeration. As demonstrated in the first part of this study [2], the excess of lung tissue, although disseminated within the overall lung parenchyma, is observed predominantly in the upper lobes, while a massive loss of aeration related partly to "compression atelectasis" is constantly observed in the lower lobes. In contrast to the lower lobes, which are essentially nonaerated, the upper lobes are normally aerated in 36% of patients with ARDS, partly aerated in 41%, and nonaerated in the remaining 23%. Radiologically these morphological differences in the distribution of air within the upper lobes give the visual impression – either on CT or chest radiography – that hyperattenuated areas are lobar, diffuse, or patchy. As soon as these differences in lung morphology became obvious to us, we made the logical hypothesis that they are associated with differences in clinical characteristics, outcome, pulmonary hemodynamics, ventilation-perfusion mismatch, and respiratory mechanics. As a consequence, cardiorespiratory parameters that had been measured prospectively when the CT was performed were compared in the three groups of patients. Because differences in lung morphology were found to be associated with differences in respiratory status and outcome, we propose a new score, the ARDS Severity Score (ARDS-SS), which identifies more accurately a subgroup of patients with a high risk of mortality related to the severity of lung injury.

Methods and materials

The study population comprised the 71 patients described in part 1 of the present study [2]. ARDS was defined according to the American-European Consensus Conference on ARDS held in 1994 [1], and informed consent was obtained from the patients' next of kin. The CT findings of 23 of these patients have been partially reported in five recently published studies [3, 4, 5, 6, 7]. Patients were classified as having primary or secondary ARDS based on history, clinical presentation, and pulmonary microbiological results by an independent observer, blinded as to the results of cardiorespiratory measurements. ARDS due to bronchopneumonia, lung contusion, and aspiration were considered as of primary origin. ARDS secondary to septic shock, intra-abdominal sepsis, and extracorporeal circulation were considered as of secondary origin.

During the study period, all patients were anesthetized and ventilated using controlled mechanical ventilation and FIO_2 of 1 as described in part 1 [2]. The study itself consisted of hemodynamic, respiratory, lung mechanics, and CT measurements performed at zero end-expiratory pressure at an early phase of ARDS.

Hemodynamic and respiratory measurements

Methods used for measuring cardiorespiratory parameters were well defined, and measurements were performed throughout the study period according to standardized protocols followed by all investigators. Arterial and pulmonary arterial pressures were measured simultaneously using the arterial cannula and the fiberoptic pulmonary artery catheter connected to two calibrated pressure transducers (91 DPT-308; Mallinckrodt) that were zeroed and positioned at the midaxillary line. Systemic and pulmonary arterial pressures, heart rate measured from the electrocardiography, tracheal pressure measured at the proximal end of the endotracheal tube, gas flow, and tidal volume measured using a heated and calibrated Hans Rudolph 3700 pneumotachograph (Hans Rudolph, Kansas City, Mo., USA), were simultaneously and continuously recorded on a Gould ES 1000 recorder throughout the entire study period.

From 1993 to 1995 arterial and pulmonary arterial pressures, pulmonary capillary wedge pressure, right atrial pressure, tidal volume, tracheal pressure and gas flow were recorded at a paper speed of 50 mm/s. Mean arterial pressure was calculated as 1/3 SAP + 2/3 DAP. Mean pulmonary artery pressure was measured by planimetry as the mean of four measurements performed at end-expiration. Pulmonary capillary wedge pressure and right atrial pressure were also measured at end-expiration. Cardiac output was measured using the thermodilution technique, and a bedside computer that allowed the recording of each thermodilution curve (Oximetric 3 SO_2/CO Computer). Four serial injections of 10 ml 5% dextrose solution at room temperature performed at random during the respiratory cycle were used to avoid errors related to the use of cold thermodilution injectate and to average the variations in cardiac output related to the inspiratory and expiratory phases of continuous positive pressure ventilation [8, 9].

During the period 1996 and 1997 signals were recorded at a high sample rate of 100 Hz on a data acquisition and analysis system including MP100 WS data acquisition system (Biopac Systems, Goleta, Calif., USA) and a Quadra 610 Macintosh computer (Apple Computer, Cupertino, Calif., USA) connected to the analog part of the hemodynamic monitor Merlin (Hewlett-Packard, Palo Alto, Calif., USA). Using the software AcqKnowledge included in the MP100 WS system, heart rate, mean arterial pressure, mean pulmonary artery pressure, pulmonary capillary wedge pressure and right atrial pressure were measured. Cardiac output was measured using the semicontinuous thermodilution technique (CCO/SvO2/VIP TD catheter).

Systemic and pulmonary arterial blood samples were taken simultaneously within 1 min after the measurement of cardiac output (after discarding an initial 10-ml heparin-contaminated aliquot). Arterial pH, arterial oxygen pressure (PaO_2), venous oxygen pressure (PvO_2), and arterial carbon dioxide pressure ($PaCO_2$) were measured using an IL BGE blood gas analyzer. Hemoglobin concentration, methemoglobin concentration, and arterial (SaO_2) and mixed venous oxygen saturations (SvO_2) were measured using a calibrated OSM3 hemoximeter. Arterial and mixed venous blood samples that showed hemoglobin concentrations differing by more than 0.1 g/100 ml were considered accidentally diluted, and the higher hemoglobin concentration was used to calculate oxygen contents. Standard formulas were used to calculate cardiac index, pulmonary vascular resistance index, systemic vascular resistance index, right stroke work index, true pulmonary shunt (Qs/Qt), arteriovenous oxygen difference, oxygen delivery, oxygen extraction ratio, and oxygen consumption.

Lung mechanics measurements

PV curves were measured using a 1-l syringe (Model Series 5540, Hans Rudolph) as previously described [10]. The endotracheal tube was disconnected from the ventilator to allow functional residual capacity (FRC) to be reached; then 100 ml increments of O_2 were given with a 2-s pause at the end of each injection. Airway pressures on inflation were recorded on the Gould ES 1000 polygraph and/or on the MP100 WS data acquisition system. A PV curve was constructed after measuring the plateau pressure for each volume increment and subtracting the pressure determined at zero volume. This allowed the determination of (a) static respiratory compliance (C_{rs}) computed as the slope of the curve after the lower inflection [10], (b) quasistatic respiratory compliance as described by Gattinoni et al. [11], (c) starting compliance (C_{start}) computed as the ratio between the first 100 ml inflation and the corresponding pressure, and (d) the lower inflection point computed as the pressure corresponding to the intersection between C_{start} and C_{rs} lines according to the method described by Gattinoni et al. [11]. Intrinsic PEEP was measured using the expiratory pause function of the César ventilator. Using the end-inspiratory pause function of the César ventilator, respiratory resistance was calculated by dividing the difference between peak inspiratory and plateau airway pressures by the previous constant inspiratory flow [12].

High-resolution and spiral thoracic CT

The method used for performing high-resolution and spiral thoracic CT is described in detail in part 1 of the present study [2]. Lung scanning was performed from the apex to the diaphragm after the intravenous injection of 80 ml contrast medium aimed at differentiating pleural effusion from nonaerated lung parenchyma as previously described [5]. CT acquisition was performed in zero end-expiratory pressure and recorded on an optical disk. Each patient was classified by an independent radiologist (P.C.), unaware of the clinical conditions of the patient, in one of the three groups according to definitions given in part 1 [2]: those with lobar attenuations, those with diffuse attenuations, and those with patchy attenuations. The patients in these three groups were similar regarding age, sex ratio, delay before inclusion, Simplified Acute Physiological Score II, duration of ventilation, length of stay in the intensive care unit, and incidence of past history of chronic obstructive pulmonary disease.

The volumes of gas and tissue were measured using a method previously described [5, 7, 13] and based on the close correlation between CT attenuation (expressed as the CT value) and physical density [14]. For each lung region of interest, the total volume, volume of gas and tissue, and fraction of gas were computed using equations provided in part 1 [2]. The lung volume (gas + tissue) at end-expiration was defined as end-expiratory lung volume. The volume of gas present in both lungs at end-expiration was defined as FRC.

Calculation of an index of hypoxic pulmonary vasoconstriction

Qs/Qt is defined as the proportion of pulmonary blood flow that perfuses nonventilated lung areas and depends both on the extension of nonventilated lung areas and the quality of hypoxic pulmonary vasoconstriction. CT analysis allows the proportion of the lung that is nonventilated to be determined, and the Swan-Ganz catheter allows the calculation of Qs/Qt. By computing the ratio between the percentage of nonventilated lung and Qs/Qt, an index of the efficiency of hypoxic pulmonary vasoconstriction (EF_{HPV}) can be obtained that does not take into account the normal gravitational inhomogeneity of perfusion. An EF_{HPV} less than 1 indicates a lack or an impairment of hypoxic vasoconstriction and a value greater than 1 the presence of hypoxic vasoconstriction. In other words, the higher the EF_{HPV}, the more efficient the hypoxic pulmonary vasoconstriction is.

Bedside chest radiography

A frontal bedside chest radiograph was obtained within 12 h of the CT acquisition. In an attempt to reproduce the CT classification, each chest radiograph was classified by the same radiologist (P.C.), blinded to the CT classification. Classification of the chest radiograph was as follows: "lobar" if hyperattenuations areas involved essentially the lower lobes; "diffuse" if hyperattenuated areas were equally disseminated within the upper and lower lobes, presenting the characteristic feature of "white lungs"; "patchy" if hyperattenuated areas involved the upper and lower lobes with a persistent aeration of a part of the upper lobes.

Statistical analysis

Comparisons between groups were performed by a one-way analysis of variance for one grouping factor followed by Fisher's probabilistic least significant difference post hoc comparison test for continuous variables and by the χ^2 test for discontinuous variables. Correlation between CT and physiological data was determined by linear regression analysis. All data in the text and tables are presented as mean ± SD unless otherwise specified. Multivariate analysis was performed on variables found to differ between survivors and nonsurvivors using a univariate analysis. The statistical analysis was performed using Statview 4.0.2 and SuperANOVA statistical software (Abacus Concepts, Berkeley, Calif., USA). The level of statistical significance was set at $p \leq 5$.

Results

Clinical characteristics of the patients

As shown in Table 1, ARDS was more frequently of primary origin in patients with diffuse and patchy attenuations and more frequently of secondary origin in patients with lobar attenuations. Lung Injury Severity Score (LISS) [15] was higher in patients with diffuse and patchy attenuations than in patients with lobar attenuations. Surgical procedures were performed more frequently in patients with lobar attenuations than in those with diffuse attenuations.

Differences between primary and secondary ARDS

Age (63 ± 13 vs. 53 ± 18 years), C_{rs} (65 ± 22 vs. 55 ± 15 ml/cmH_2O), and PaO_2 (111 ± 52 vs. 86 ± 33 mmHg) were slightly higher in patients with secondary than with primary ARDS ($p < 0.05$). Otherwise, all the parameters measured, including mortality (53% vs.

Table 1 Demographic data of the three groups of patients (*LA* lobar attenuations, *DA* diffuse attenuations, *PA* patchy attenuations, *ECC* extracorporeal circulation, *MV* mechanical ventilation; *Delay* time between the onset of ARDS and cardiorespiratory measurements)

	LA (n = 26)	DA (n = 16)	PA (n = 29)	p[a]
Age (years)	60 ± 16	54 ± 15	55 ± 18	NS
Sex ratio (M/F)	23/3	10/6	26/3	NS
Delay (days)	4 ± 2	5 ± 4	4 ± 2	NS
Survivors	15 (58%)	4 (25%)	17 (59%)	0.05
ASA score	2 ± 1	2 ± 1	2 ± 1	NS
SAPS II	40 ± 12	44 ± 14	37 ± 12	NS
LISS	2.3 ± 0.4	3.5 ± 0.2*	3.0 ± 0.3*,**	0.001
Duration of MV	46 ± 39	36 ± 26	37 ± 32	NS
ICU duration	45 ± 37	37 ± 38	39 ± 37	NS
Primary ARDS	13 (50%)	13 (82%)	23 (79%)	0.03
Bronchopneumonia	13	9	14	
Lung contusion	0	3	4	
Aspiration	1	2	4	
Secondary ARDS	12 (46%)	2 (12%)	6 (21%)	0.03
Extra-abdominal sepsis	9	2	6	
Intra-abdominal sepsis	0	1	0	
ECC	5	0	0	
ARDS of both origins	1 (4%)	1 (6%)	0	
Surgery	22 (85%)	7 (44%)	17 (58%)	0.001
Multiple trauma	3 (12%)	5 (31%)	12 (42%)	0.001
Medical disease	1 (3%)	4 (25%)	0	0.001

* $p < 0.05$ vs. patients with lobar attenuations, ** $p < 0.05$, vs. patients with diffuse attenuations

[a] The p value of the grouping factor using one-way analysis of variance

Table 2 Respiratory parameters in the three groups of patients (FIO_2 = 1, PEEP = 0; *LA* lobar attenuations, *DA* diffuse attenuations, *PA* patchy attenuations, SvO_2 mixed venous oxygen saturation, Qs/Qt pulmonary shunt, DO_2I oxygen delivery index, VO_2I oxygen consumption index, EaO_2 oxygen extraction ratio, $C\ (a\text{-}v)O_2$ arteriovenous oxygen difference, V minute ventilation)

	LA (n = 26)	DA (n = 16)	PA (n = 29)	p[a]
PaO_2 (mmHg)	110 ± 39	76 ± 42*	82 ± 30*	0.004
Hemoglobin (g dl^{-1})	10.2 ± 2.0	9.3 ± 1.3	9.3 ± 1.6	NS
PvO_2 (mmHg)	40.8 ± 8.8	38.2 ± 5.2	38.2 ± 5.2	NS
SvO_2 (%)	69.4 ± 10.2	64.7 ± 16.0	67.3 ± 9.0	NS
Qs/Qt (%)	41.7 ± 11.2	47.3 ± 8. 9*	47.3 ± 8.9*	0.011
DO_2I (ml min^{-1} m^{-2})	423 ± 107	447 ± 179	475 ± 175	NS
VO_2I (ml min^{-1} m^{-2})	111 ± 36	124 ± 49	125 ± 42	NS
EaO_2 (%)	27.1 ± 8.6	29.9 ± 10.8	27.8 ± 7.9	NS
C (a-v)O_2 (vol/100 ml)	3.6 ± 1.1	3.1 ± 0.7	3.1 ± 0.8	NS
$PaCO_2$ (mmHg)	42 ± 6	49 ± 11*	47 ± 8	0.047
V (l min^{-1})	12 ± 2.7	14 ± 3.6	12 ± 2**	NS

*$p < 0.05$ vs. patients with lobar attenuations, ** $p < 0.05$ vs. patients with diffuse attenuations

[a] The p value of the grouping factor using one-way analysis of variance

50%), hemodynamic, respiratory and CT parameters, were similar between primary and secondary ARDS.

Differences in respiratory status between the respective groups

As shown in Table 2, arterial oxygenation was less impaired in patients with lobar attenuations than in those with diffuse or patchy attenuations because of a lower true intrapulmonary shunt. As shown in Fig. 1, hypoxic pulmonary vasoconstriction was severely impaired in the three groups of patients and independently of the differences in lung morphology: in 84% of patients EF_{HPV} was less than 1, suggesting not only the lack of pulmonary vasoconstriction in nonventilated areas but also some degree of vasodilation. In a minority of patients with patchy and diffuse attenuations EF_{HPV} was greater than 1 suggesting a predominant distribution of pulmonary blood flow towards aerated lung regions. Only one patient with lobar attenuations had an EF_{HPV} greater than 1, suggesting a virtually absent HPV in this category of patient. Patients with diffuse attenuations had a significantly higher $PaCO_2$ than patients of the two other groups. All the other respiratory parameters were similar between groups.

Differences in respiratory mechanics and PV curves between the three groups are presented in Table 3. Patients with diffuse attenuations had the lowest quasistatic and starting respiratory compliances and the highest

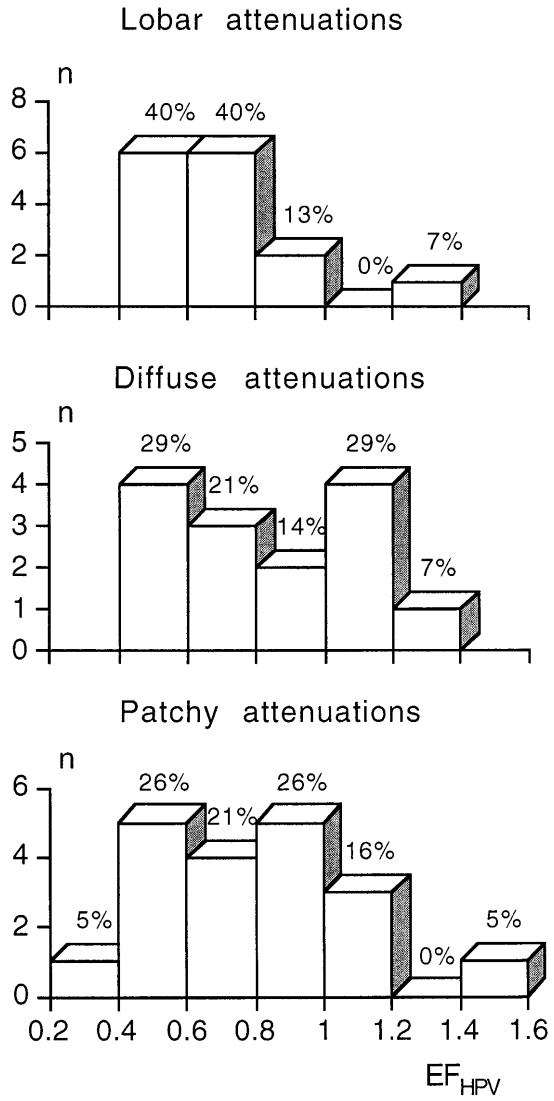

Fig. 1 Distribution of the index of efficiency of hypoxic pulmonary vasoconstriction (EF_{HPV}) computed as the ratio between the percentage of nonventilated lung and Qs/Qt in the three groups of patients. $EF_{HPV} = 1$ indicates a lack of hypoxic pulmonary vasoconstriction; $EF_{HPV} < 1$ indicates a predominant vasodilation in nonaerated lung areas; $EF_{HPV} > 1$ indicates a predominant vasoconstriction in nonaerated lung areas. *Y-axis* Number of patients (*n*); *X-axis* EF_{HPV} value

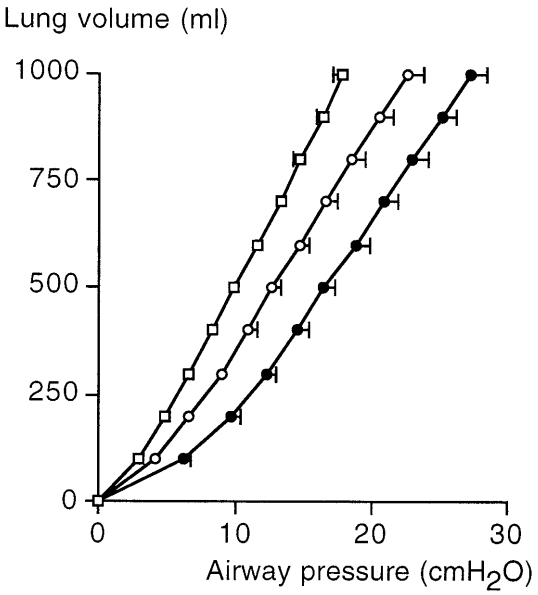

Fig. 2 Pressure-volume (PV) curves obtained at zero end-expiratory pressure in 26 patients with lobar attenuations (*open squares*), 29 with patchy attenuations (*open circles*), and 16 with diffuse attenuations (*filled circles*). The three PV curves are significantly different from each other. Data are mean ± SEM

peak inspiratory airway pressure and the lowest inflection point and C_{rs}/C_{start} ratio. On the other hand, patients with lobar attenuations had the highest quasistatic, static and starting respiratory compliances and the lowest peak inspiratory airway pressure, and the lowest inflection point and C_{rs}/C_{start} ratio. As shown in Fig. 2, the PV curves of the patients with diffuse attenuations were shifted to the right compared to the two other groups. This was due to the presence of a marked lower inflection point on the PV curve of every patient of this group. In contrast, the PV curves of patients with lobar attenuations were shifted to the left and nearly linear. In 85 % of patients with lobar attenuations the lower inflection point was 5 cmH_2O or lower, while in 90 % of patients with diffuse attenuations the lowest inflection point was 7 cmH_2O or higher. Respiratory resistance and intrinsic PEEP did not differ significantly between groups.

Differences in hemodynamics between the respective groups

As shown in Table 4, except concerning some slight differences in heart rate the three groups were comparable for all systemic and pulmonary hemodynamic parameters.

Correlations between loss of aeration, excess of lung tissue, and cardiorespiratory parameters

As shown in Fig. 3, PaO_2 and Qs/Qt were not correlated with the amount of lung tissue in excess. In contrast, both parameters were correlated, although not closely, with FRC. Mean pulmonary artery pressure and pulmonary vascular resistance were not correlated with the amount of lung tissue in excess.

Table 3 Lung mechanics in the three groups of patients ($FIO_2 = 1$ and PEEP = 0; *LA* lobar attenuations, *DA* diffuse attenuations, *PA* patchy attenuations, P_{max} peak inspiratory airway pressure, C_{qs} quasistatic respiratory compliance, C_{rs} slope of the PV curve in its linear part, *LIP* lower inflection point, *Rrs* respiratory resistance, *PEEPi* intrinsic PEEP)

	LA ($n = 26$)	DA ($n = 16$)	PA ($n = 29$)	p^a
Respiratory rate (min^{-1})	18 ± 3	24 ± 5*	19 ± 5**	0.005
Tidal volume (ml)	704 ± 123	631 ± 170	663 ± 120	NS
P_{max} (cmH_2O)	21.3 ± 6.1	29.9 ± 11.0*	24.1 ± 6.4**	0.004
C_{qs} (ml cmH_2O^{-1})	59 ± 30	37 ± 10*	48 ± 15*	0.005
C_{rs} (ml cmH_2O^{-1})	64 ± 16	47 ± 12*	56 ± 18	0.039
C_{start} (ml cmH_2O^{-1})	41 ± 21	19 ± 9*	30 ± 15*	0.001
C_{rs}/C_{start} ratio	1.8 ± 0.6	2.8 ± 0.9*	2.3 ± 1.3	0.009
Inflection point present	19 (73%)	16 (100%)	22 (76%)	
LIP (cmH_2O)	4.6 ± 2.0	8.4 ± 2.0*	6.3 ± 2.7*,**	0.001
Rrs ($cmH_2O^{-1}\ l^{-1}\ s^{-1}$)	6.3 ± 3.7	6.7 ± 2.8	7.2 ± 3.0	NS
PEEPi (cmH_2O^{-1})	1.9 ± 1.8	2.7 ± 2.2	3.2 ± 3.3	NS

* $p < 0.05$ vs. patients with lobar attenuations, ** $p < 0.05$ vs. patients with diffuse attenuations
[a] The p value of the grouping factor using one-way analysis of variance

Table 4 Hemodynamic parameters in the three groups of patients ($FIO_2 = 1$ and PEEP = 0; *LA* lobar attenuations, *DA* diffuse attenuations, *PA* patchy attenuations, *MPAP* mean pulmonary arterial pressure, *PVRI* pulmonary vascular resistance index, *RAP* right atrial pressure, *RVSWI* right ventricular stroke work index, *MAP* mean arterial pressure, *SVRI* systemic vascular resistance index, *HR* heart rate, *PCWP* pulmonary capillary wedge pressure, *SVI* stroke volume index, *CI* cardiac index)

	LA ($n = 26$)	DA ($n = 16$)	PA ($n = 29$)	p^a
MPAP (mmHg)	27 ± 9	29 ± 7	29 ± 8	NS
PVRI (dyne $s^{-1}\ cm^{-5}\ m^{-2}$)	473 ± 283	404 ± 181	446 ± 333	NS
RAP (mmHg)	8.3 ± 4.3	8.5 ± 4.7	7.5 ± 4.2	NS
RVSWI (g m^{-2})	10.1 ± 5.0	11.3 ± 4.2	11.9 ± 5.5	NS
MAP (mmHg)	82 ± 15	81 ± 16	79 ± 14	NS
SVRI (dyne $s^{-1}\ cm^{-5}\ m^{-2}$)	1995 ± 680	1635 ± 671	1570 ± 734	NS
PCWP (mmHg)	9.3 ± 4.5	10.1 ± 4.4	8.9 ± 4.1	NS
HR (min^{-1})	87 ± 19	99 ± 18*	99 ± 18*	0.036
CI (l $min^{-1}\ m^{-2}$)	3.2 ± 1.2	4.1 ± 1.7	4.2 ± 1.7	NS

* $p < 0.05$ vs. patients with lobar attenuations
[a] The p value of the grouping factor using one-way analysis of variance

As shown in Fig. 4, the FRC (expressed in liters) was inversely correlated with P_{max} ($P_{max} = -7x + 31$; $r = 0.43$, $p = 0.001$) and the value of the lower inflection point ($p = 0.0001$) and was correlated with C_{start} ($C_{start} = 21x + 12$; $r = 0.50$, $p = 0.0002$), C_{rs} ($C_{rs} = 16x + 42$; $r = 0.38$, $p = 0.07$) and C_{qs} ($p = 0.0001$). In contrast, the volume of lung tissue was not correlated with any of these parameters.

Comparison of radiographic and CT classifications

Figure 5 shows the ability of frontal bedside chest radiography to identify patients with lobar, diffuse, and patchy attenuations according to CT features. Of the 71 patients only 30 were correctly classified by the bedside chest radiography. The discrepancy between chest radiographic and CT classifications was the lowest in patients with diffuse attenuations.

Factors affecting outcome and definition of ARDS-SS

Overall mortality was 46%; it was higher in patients with diffuse attenuations (75%) than in those with lobar and patchy attenuations (41 and 42%). As shown in Table 5, only age, starting compliance, C_{rs}/C_{start} ratio, and intrinsic PEEP differed significantly between survivors and nonsurvivors. Multivariate analysis showed that only C_{rs}/C_{start} ratio independently associated with mortality.

To better predict mortality resulting from the severity of the lung injury, we propose two new scores based on radiography and CT in ZEEP conditions. Table 6 shows the various parameters involved in the CT-based ARDS-SS and the number of points corresponding to a given value of each item. Table 7 shows the various parameters involved in the Chest Radiography-based Severity Score and the number of points corresponding to a given value of each item. Figure 6 shows the mortality rate observed in our series of patients according to

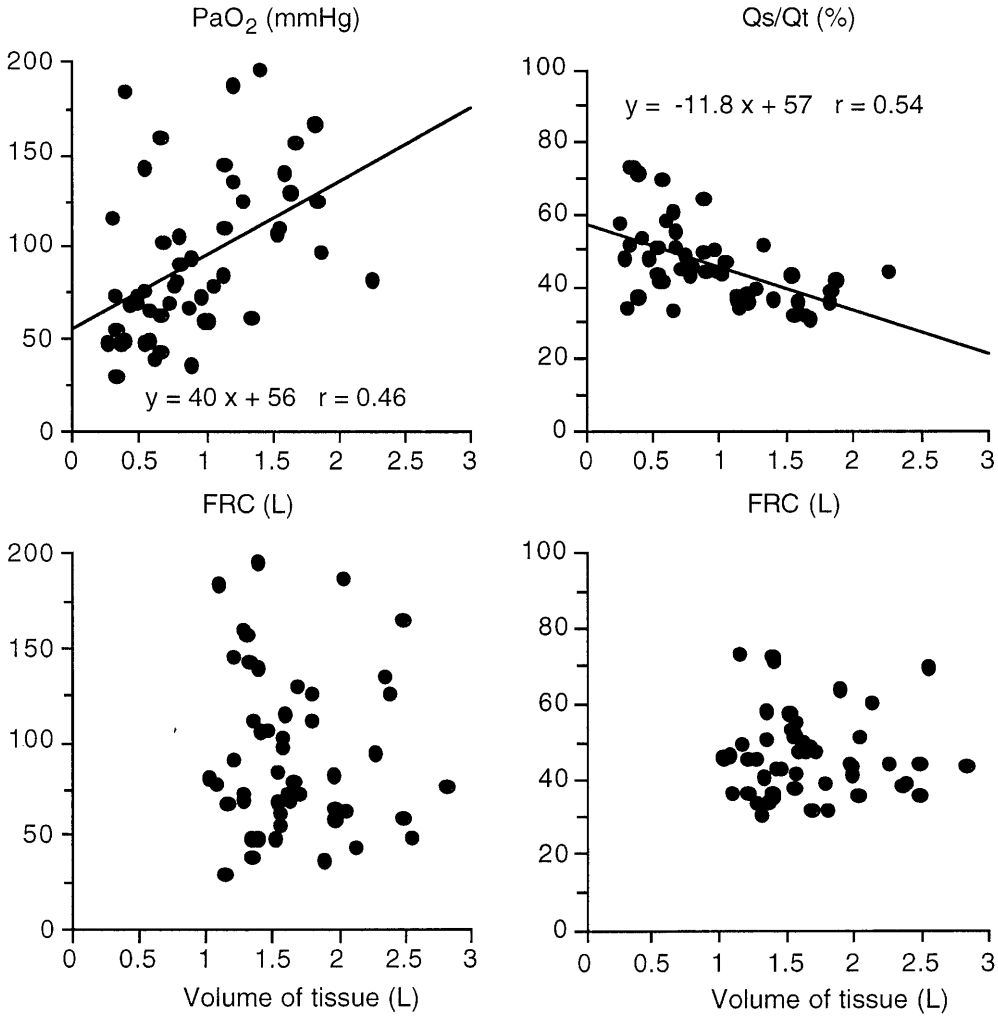

Fig. 3 PaO_2 and Qs/Qt are correlated to the functional residual capacity (*FRC*); *upper*) but not to the volume of tissue (*lower*) in 48 patients with ARDS (ZEEP conditions)

LISS, Chest Radiography-based Severity Score and CT-based ARDS-SS. Only the ARDS-SS was able to identify patients with a mortality rate above 75%. The three scores differed significantly between survivors and non-survivors only when adjusted for age. Patients with diffuse attenuations had a mean ARDS-SS of 16 ± 3, corresponding to a mortality rate of 75%, those with lobar attenuations had a mean ARDS-SS of 5 ± 2, corresponding to a mortality rate of 42%, and those with patchy attenuations had a mean ARDS-SS of 10 ± 3, corresponding to a mortality rate of 41%. These differences were highly significant ($p < 0.001$). The corresponding values on the Chest Radiography-based Severity Score were 9 ± 3, 9 ± 2, and 12 ± 2.

Discussion

This study demonstrates that differences in lung morphology are associated with differences in the cause of ARDS, mortality rate, and lung mechanics. Among a large series of patients fulfilling the criteria of ARDS, three groups were defined according to differences in lung morphology evidenced on CT. In 23% of patients there were diffuse and bilateral hyperattenuated areas. These patients had marked alterations in lung mechanics characterized by a marked inflection point on the initial part of the PV curve and a low compliance of the respiratory system, a mortality rate of 75%, and a primary origin for their ARDS. In 36% there were nondiffuse bilateral hyperattenuated areas, predominantly in the lower lobes. In this group mortality rate was 42%, the alterations in respiratory mechanics were moderate, with a lower inflection point that was absent or lower than 5 cmH_2O, and ARDS was more frequently of secondary origin (in 44% of the patients). In 41% there were bilateral patchy hyperattenuated areas. Alterations in respiratory mechanics were comparable to those observed in patients with diffuse attenuations, although mortality rate was identical to the mortality rate of pa-

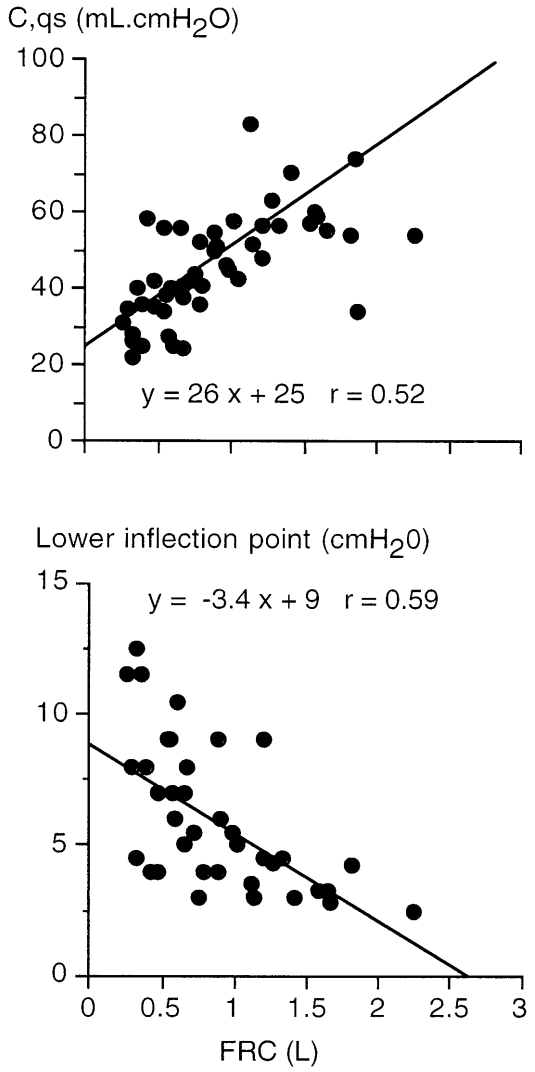

Fig. 4 Correlations between the functional residual capacity (*FRC*) and the quasistatic compliance (*upper*) and the value of the lower inflection point (*lower*) in 48 patients with ARDS (ZEEP conditions)

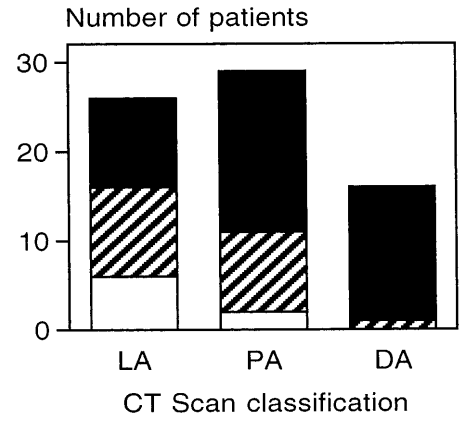

Fig. 5 Comparison of radiographic and CT classifications: number of patients with chest radiography classified as lobar (*white bars*), patchy (*hatched bars*), and diffuse (*black bars*). Bedside chest radiography identified all patients with diffuse attenuation but misclassified patients with lobar and patchy attenuations. *LA* Lobar attenuations; *PA* patchy attenuations; *DA* diffuse attenuations according to CT classification

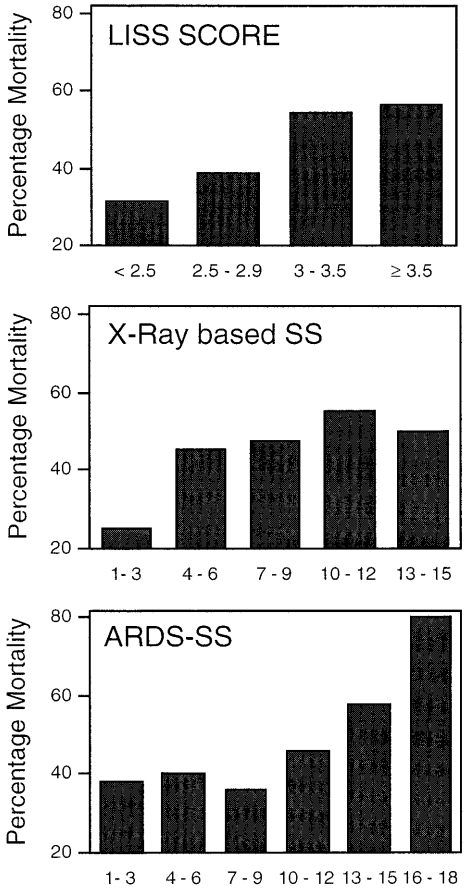

Fig. 6 Mortality rate according to the LISS (*upper*), bedside Chest Radiography-based Severity Score (*middle*), and ARDS Severity Score (*lower*). Only the ARDS Severity Score identified the patients having a mortality above 60%

tients with lobar attenuations. In this group of patients ARDS was mainly of primary origin. In all three groups of patients, arterial oxygenation was severely impaired but significantly less so in patients with lobar attenuations than those of the other two groups. Based on these results we proposed a new scoring system, the ARDS-SS, which gives specific weight to CT features and to alterations in lung mechanics. In contrast to the LISS and to the Chest Radiography-based Severity Score, this new score identifies the patients with the most severe ARDS, having a mortality rate above 60% (Fig. 6).

The ARDS-SS takes into account the PaO_2/FIO_2 ratio, two characteristics of the PV curve – the lower inflection point and the slope of the curve – lung morphol-

Table 5 Comparison between survivors and nonsurvivors (FIO_2 100 % without PEEP; P_{max} peak inspiratory airway pressure, C_{qs} quasistatic respiratory compliance, C_{rs} slope of the PV curve in its linear part, C_{start} starting compliance, *LIP* lower inflection point, *Rrs* respiratory resistance, *PEEPi* intrinsic PEEP, *SPAP* systolic pulmonary artery pressure, *MPAP* mean pulmonary arterial pressure, *DPAP* diastolic pulmonary artery pressure, *PVRI* pulmonary vascular resistance index, *RAP* right atrial pressure, *RVSWI* right ventricular stroke work index, *MAP* mean arterial pressure, *SVRI* systemic vascular resistance index, *PCWP* pulmonary capillary wedge pressure, *HR* heart rate, *CI* cardiac index, arterial O_2 pressure, venous O_2 pressure, SvO_2 mixed venous oxygen saturation, *Qs/Qt* pulmonary shunt, DO_2I oxygen delivery index, VO_2I oxygen consumption index, EaO_2 oxygen extraction ratio, $C\ (a\text{-}v)O_2$ arteriovenous oxygen difference, arterial CO_2 pressure, *V* minute ventilation)

	Survivors ($n = 36$)	Nonsurvivors ($n = 35$)	*p*
Age (years)	52 ± 19	61 ± 14	0.02
Primary ARDS	26 (72 %)	25 (71 %)	NS
P_{max} (cmH_2O)	24 ± 10	24 ± 7	NS
C_{qs} (ml cmH_2O^{-1})	50 ± 16	49 ± 28	NS
C_{rs} (ml cmH_2O^{-1})	57 ± 18	57 ± 16	NS
C_{start} (ml cmH_2O^{-1})	38 ± 22	24 ± 10	0.002
C_{rs}/C_{start} ratio	1.8 ± 0.8	2.6 ± 1.2	0.001
Inflection point present	25 (70 %)	35 (100 %)	0.0001
LIP (cmH_2O)	6.3 ± 2.9	6.3 ± 2.6	NS
Rrs (cmH_2O^{-1} L^{-1} s^{-1})	6.9 ± 3.1	6.6 ± 3.5	NS
PEEPi (cmH_2O^{-1})	1.6 ± 1.6	3.6 ± 3.0	0.002
SPAP (mmHg)	43 ± 13	42 ± 13	NS
MPAP (mmHg)	28 ± 9	28 ± 8	NS
DPAP (mmHg)	20 ± 7	19 ± 7	NS
PVRI (dyne s^{-1} cm^{-5} m^2)	439 ± 321	455 ± 243	NS
RAP (mmHg)	8 ± 4	8 ± 5	NS
RVSWI (g m^{-2})	12 ± 6	10 ± 3	NS
RVSWI/VSWI	0.25 ± 0.13	0.32 ± 0.17	0.06
MAP (mmHg)	84 ± 16	77 ± 14	NS
SVRI (dyne s^{-1} cm^{-5} m^2)	1823 ± 828	1654 ± 584	NS
PCWP (mmHg)	9 ± 4	10 ± 5	NS
HR (min^{-1})	95 ± 21	95 ± 19	NS
CI (l min^{-1} m^{-2})	3.9 ± 1.7	3.7 ± 1.5	NS
PaO_2 (mmHg)	95 ± 36	87 ± 41	NS
Hb (g dl^{-1})	9.4 ± 1.8	9.9 ± 1.7	NS
PvO_2 (mmHg)	39 ± 6	40 ± 8	NS
SvO_2 (%)	68 ± 9	67 ± 14	NS
Qs/Qt (%)	44 ± 8	48 ± 13	NS
DO_2I (ml min^{-1} m^{-2})	457 ± 157	441 ± 152	NS
VO_2I (ml min^{-1} m^{-2})	122 ± 36	118 ± 47	NS
EaO_2 (%)	28 ± 7	28 ± 10	NS
C (a-v)O_2 (vol/100 ml)	3.2 ± 0.8	3.3 ± 1.1	NS
$PaCO_2$ (mmHg)	44 ± 7	48 ± 10	0.04
V (l min^{-1})	12 ± 2	13 ± 5	NS

Table 6 CT-based ARDS Severity Score (ZEEP conditions)

Parameter	Range	Number of points
PaO_2/FIO_2 ratio	150–200 mmHg	0
	100–150 mmHg	1
	50–100 mmHg	2
	< 50 mmHg	3
Lower inflection point	Absent	0
	< 5 cmH_2O	1
	5–10 cmH_2O	2
	> 10 cmH_2O	3
Slope of the PV curve	> 60 ml/cmH_2O	0
	50–60 ml/cmH_2O	1
	40–50 ml/cmH_2O	2
	< 40 ml/cmH_2O	3
CT feature	Lobar attenuations	0
	Patchy attenuations	3
	Diffuse attenuations	5
Proportion of aerated lung	> 50 %	0
	40–50 %	2
	30–40 %	4
	30 %	6

Table 7 Chest Radiography-based Severity Score (ZEEP conditions)

Parameter	Range	Number of points
PaO_2/FIO_2 ratio	150–200 mmHg	0
	100–150 mmHg	1
	50–100 mmHg	2
	< 50 mmHg	3
Lower inflection point	Absent	0
	5 cmH_2O	1
	5–10 cmH_2O	2
	10 cmH_2O	3
Slope of the PV curve	60 ml/cmH_2O	0
	50–60 ml/cmH_2O	1
	40–50 ml/cmH_2O	2
	40 ml/cmH_2O	3
Bedside chest radiograph	Lobar attenuations	0
	Patchy attenuations	3
	Diffuse attenuations	6

ogy, and the proportion of aerated lung measured at zero end-expiratory pressure, all indices of severe lung injury associated with poor outcome. According to two recent studies [16, 17], only a severe impairment of arterial oxygenation (defined as a PaO_2/FIO_2 less than 150 mmHg) is considered potentially to have an effect on outcome. In the present study, oxygenation parameters were correlated with FRC and not with the excess of lung tissue, as previously reported [13]. The lack of correlation between excess of lung tissue and impairment of arterial oxygenation is likely due to the fact that the fall in PaO_2 depends mainly on the perfusion of nonventilated areas, which in turn is determined predominantly by three factors: the proportion of lung area remaining aerated, quality of the hypoxic pulmonary vasoconstriction, and hemodynamic status. In more than 75 % of the patients enrolled in the present study hypoxic pulmonary vasoconstriction was severely impaired (Fig. 1), rendering the PaO_2 dependent essentially on the volume of lung remaining aerated. All patients with lobar attenuations except one had a severe impairment of hypoxic pulmonary vasoconstriction, rendering

unlikely the hypothesis that the excess of lung tissue present in the upper lobes is related principally to the redistribution of pulmonary blood flow towards these lobes (see part 1 [2]). It must be pointed out that the amount of lung tissue in excess was not correlated with any of the markers of the pulmonary vascular disease such as pulmonary artery pressure and pulmonary vascular resistance. This absence of correlation is not surprising and indicates that lung inflammation and pulmonary edema do not compress pulmonary vessels sufficiently to play a role in the increase in pulmonary vascular resistance observed in ARDS, the pulmonary hypertension resulting mainly from active vasoconstriction, microvascular clotting, and vascular remodeling [18]. In other words, the pulmonary vascular disease observed in ARDS appears to be dissociated from the alveolar disease. These results are not consistent with the data of Gattinoni et al. [13], who have reported a close correlation between lung tissue in excess, impairment of PaO_2, and increase in pulmonary artery pressure. The two likely explanations for this discrepancy are the larger number of patients included in our study and the differences in the method for measuring the volume of lung tissue. In the Gattinoni et al. study the volume of lung tissue was inferred from the simultaneous measurements of FRC and mean lung attenuation. FRC was measured by the helium dilution technique, which is known to be lacking in precision in patients with ARDS (see "Discussion" in part 1 [2]). The mean lung attenuation was obtained by measuring the mean CT value on three CT sections performed at the apex, the hilum, and the lung base, and it was assumed that these three CT sections are representative of the entire lung parenchyma. The data reported in part 1 [2] demonstrate that this assumption is not always valid, particularly in patients with lobar attenuations.

The different compliances measured in the present study (static, quasistatic, and starting compliances) were significantly correlated with FRC but not with the amount of lung tissue. These data confirm the previous study of Gattinoni et al. [11] who first reported that the alterations in lung mechanics are related to the decrease in the volume of aerated lung. Confirming a recent study [7], our results demonstrate that the presence of a lower inflection point, greater than 5 cmH_2O, on the initial part of the PV curve is associated with an homogeneous distribution of the loss of aeration in the diseased lungs. In addition, the value of the lower inflection point was inversely correlated with the FRC (Fig. 4). Lobar attenuations observed were predominantly found in patients without or with a lower inflection point(< 5 cmH_2O). It has recently been demonstrated that the presence of such a low lower inflection point is often related to chest wall compliance abnormalities rather than to alterations in mechanical properties of the lung parenchyma [19].

Because patients with lobar attenuations demonstrated less severe alterations in the PV curve and lower mortality than those with diffuse attenuations, the following parameters were considered as criteria of severity in the ARDS-SS: respiratory compliance less than 60 ml/cmH_2O, lower inflection point greater than 5 cmH_2O, and the presence of diffuse attenuations. FRC reduced by more than 50 % was considered as an additional criteria of severity. As noted above, the three groups did not differ regarding the pulmonary vascular disease. Furthermore, pulmonary artery pressure was similar in survivors and nonsurvivors. As a consequence, and despite the fact that a recent study has shown that mean pulmonary artery pressure is slightly higher in nonsurvivors than in survivors [16], none of the pulmonary hemodynamic parameters were included in the ARDS-SS.

Neither LISS nor ARDS-SS values differed significantly between survivors and nonsurvivors when analyzed independently of confounding variables such as age, which was identified very early as a major determinant of outcome in ARDS [20]. This result is in accordance with the findings of two large studies on mortality in ARDS in which the LISS was similar in survivors and nonsurvivors [17, 21]. This indicates that mortality in ARDS patients depends not only upon the severity of lung injury but also on the underlying disease, the physiological condition, and the other organ dysfunctions [16, 17]. Mortality increased with the score of both LISS and ARDS-SS. However, only ARDS-SS, based partly upon the analysis of CT features, discriminated patients with a mortality rate higher than 60 % (Fig. 6). Further studies are required to validate ARDS-SS prospectively in large series of patients with ARDS.

Two items of the ARDS-SS are based on analysis of the CT image. This raises the critical question of whether CT of the entire lung should be systematically performed during the early phase of ARDS. Because differences in lung morphology are associated with different outcome and different strategies of alveolar recruitment (see part 3 [22]), it seems of clinical relevance to accurately assess the distribution of loss of aeration within lung parenchyma. The present study clearly shows that bedside chest radiography frequently results in erroneous evaluation of the distribution of gas and tissue within the diseased lung parenchyma. Neither LISS nor the Chest Radiography-based Severity Score accurately identified the subgroups of patients with a high mortality rate. This is likely due to the poor quality of bedside chest radiography, especially in the intensive care environment. Software as Lungview may become available in the near future in departments of radiology, making possible an accurate assessment of lung morphology and the measurements of lung volumes. When carried out correctly, the transportation of the patient

to the radiology department does not pose a real problem. Our experience with several hundreds of patients indicate that very ill patients, when correctly monitored, ventilated, and accompanied by skilled physicians, can be safely transported outside the intensive care unit.

In conclusion, differences in lung morphology were associated with differences in lung mechanics, arterial oxygenation, cause of ARDS and mortality rate. Patients with diffuse attenuations homogeneously distributed within both lungs had marked alterations in respiratory mechanics, more frequently ARDS of primary origin, and a high mortality rate. The new ARDS-SS based on oxygenation impairment, alteration in respiratory mechanics, and lung morphology accurately identified a subgroup of patients with severe ARDS and a high mortality rate, likely requiring a specific ventilatory approach in terms of alveolar recruitment and CO_2 elimination. The effect of lung morphology on the cardiorespiratory effects of PEEP and on the strategy of alveolar recruitment is presented in part 3 [22].

References

1. Bernard GR, Artigas A, Brigham KL, Carlet J, Falke K, Hudson L, Lamy M, Legall JR, Morris A, Spragg R (1994) The American-European Consensus Conference on ARDS. Definitions, mechanisms, relevant outcomes, and clinical trial coordination. Am J Respir Crit Care Med 149: 818–824
2. Puybasset L, Cluzel P, Gusman P, Grenier P, Preteux F, Rouby J-J, CT scan ARDS study group (2000) Regional distribution of gas and tissue in acute respiratory distress syndrome. I. Consequences for lung morphology. Intensive Care Med 26: 857–869
3. Puybasset L, Rouby JJ, Mourgeon E, Cluzel P, Law-Koune JD, Stewart T, Devilliers C, Lu Q, Roche S, Kalfon P, Vicaut E, Viars P (1995) Factors influencing cardiopulmonary effects of inhaled nitric oxide in acute respiratory failure. Am J Respir Crit Care Med 152: 318–328
4. Umamaheswara Rao GS, Gallart L, Law-koune J-D, Lu Q, Puybasset L, Coriat P, Rouby JJ (1997) Factors influencing the uptake of inhaled nitric oxide in patients on mechanical ventilation. Anesthesiology 87: 823–834
5. Vieira S, Puybasset L, Richecoeur J, Lu Q, Cluzel P, Gusman P, Coriat P, Rouby JJ (1998) A lung computed tomographic assessment of positive end-expiratory pressure-induced lung overdistension. Am J Respir Crit Care Med 158: 1571–1577
6. Puybasset L, Cluzel P, Chao N, Slutsky A, Coriat P, Rouby JJ, CT Scan ARDS Study group (1998) A computed tomography assessment of regional lung volume in acute lung injury. Am J Respir Crit Care Med 158: 1644–1655
7. Vieira S, Puybasset L, Lu Q, Richecoeur J, Cluzel P, Coriat P, Rouby JJ (1999) A scanographic assessment of pulmonary morphology in acute lung injury: signification of the lower inflection point detected on lung pressure-volume. Am J Respir Crit Care Med 159: 1612–1623
8. Chioléro R, Mavrocordatos P, Bracco D, Schutz Y, Cayeux C, Revelly JP (1994) O2 consumption by the Fick method: methodologic factors. Am J Respir Crit Care Med 149: 1118–1122
9. Assmann R, Falke KJ (1988) Pressure and volume assessment of right ventricular function during mechanical ventilation. Intensive Care Med 14 [Suppl 2]:467–470
10. Lu Q, Vieira S, Richecoeur J, Puybasset L, Kalfon P, Coriat P, Rouby JJ (1999) A simple automated method for measuring pressure-volume curve during mechanical ventilation. Am J Respir Crit Care Med 159: 257–282
11. Gattinoni L, Pesenti A, Avalli L, Rossi F, Bombino M (1987) Pressure-volume curve of total respiratory system in acute respiratory failure. Computed tomographic scan study. Am Rev Respir Dis 136: 730–736
12. Bates JHT, Rossi A, Milic-Emili J (1985) Analysis of the behavior of the respiratory system with constant inspiratory flow. J Appl Physiol 58: 1840–1848
13. Gattinoni L, Pesenti A, Bombino M, Baglioni S, Rivolta M, Rossi G, Rossi F, Marcolin R, Mascheroni D, Torresin A (1988) Relationships between lung computer tomographic density, gas exchange, and PEEP in acute respiratory failure. Anesthesiology 69: 824–832
14. Mull RT (1984) Mass estimates by computed tomography: physical density from CT numbers. AJR Am J Roentgenol 143: 1101–1104
15. Murray JF, Matthay MA, Luce JM, Flick MR (1988) An expanded definition of the adult respiratory distress syndrome. Am Rev Respir Dis 138: 720–723
16. Squara P, Dhainaut JF, Artigas A, Carlet J (1998) Hemodynamic profile in severe ARDS: results of the European Collaborative ARDS Study. Intensive Care Med 24: 1018–1028
17. Monchi M, Bellenfant F, Cariou A, Joly LM, Thebert D, Laurent I, Dhainaut JF, Brunet F (1998) Early predictive factors of survival in the acute respiratory distress syndrome. A multivariate analysis. Am J Respir Crit Care Med 158: 1076–1081
18. Zapol WM, Snider MT (1977) Pulmonary hypertension in severe acute respiratory failure. N Engl J Med 296: 476–480
19. Mergoni M, Martelli A, Volpi A, Primavera S, Zuccoli P, Rossi A (1997) Impact of positive end-expiratory pressure on chest wall and lung pressure-volume curve in acute respiratory failure. Am J Respir Crit Care Med 156: 846–854
20. Gee MH, Gottlieb JE, Albertine KH, Kubis JM, Peters SP, Fish JE (1990) Physiology of aging related to outcome in the adult respiratory distress syndrome. J Appl Physiol 69: 822–829
21. Zilberberg MD, Epstein SK (1998) Acute lung injury in the medical ICU. Am J Respir Crit Care Med 157: 1159–1164
22. Puybasset L, Gusman P, Muller J-C, Cluzel P, Coriat P, Rouby J-J, CT scan ARDS study group (2000) Regional distribution of gas and tissue in acute respiratory distress syndrome. III. Consequences for the effects of positive end expiratory pressure. Intensive Care Med (in press)